

Helical Spin Order from Topological Dirac and Weyl (Semi-)Metals

Xiao-Qi Sun,¹ Zhong Wang,^{1,2,*} and Shou-Cheng Zhang^{3,1}

¹ Institute for Advanced Study, Tsinghua University, Beijing, China, 100084

² Collaborative Innovation Center of Quantum Matter, Beijing 100871, China

³ Department of Physics, Stanford University, Stanford, CA 94025

(Dated: February 15, 2019)

We study dynamical mass generation and the resultant helical spin orders in topological Dirac and Weyl (semi-)metals, including the edge states of quantum spin Hall insulators, the surface states of weak topological insulators, and the bulk materials of Weyl semimetals. In particular, the helical spin textures of Weyl semimetals manifest the spin-momentum locking of Weyl fermions in a visible manner. The spin-wave fluctuations of the helical order carry electric charge density, therefore, the spin textures can be electrically controlled in a simple and predictable manner.

PACS numbers: 73.43.-f, 71.70.Ej, 75.70.Tj

Relativistic electrons governed by the Dirac equation had been thought to be remote from condensed matter physics. The developments in the last decade, especially the discovery of graphene[1] and topological insulators[2–4], however, have established the ubiquitousness of Dirac fermions in condensed matter. The topologically protected surface states of topological insulators are generally massless Dirac fermions, meanwhile, the bulk states of many topological insulators can be described by massive Dirac equations. More recently, massless Dirac[5–7] (and Weyl[8–25]) fermions have also been discovered in bulk materials (a recent experimentally discovered material is the TaAs class[26–33]).

The interactions among the nominal massless Dirac fermions, if sufficiently strong, can dynamically generate a Dirac mass and fundamentally change the properties of fermions. This phenomenon was first studied in the context of particle physics[34]. In fact, the dominant parts of proton and neutron masses come from the dynamically generated quark masses (the bare quark masses contribute only a tiny part). In this paper we investigate the physical consequences of dynamical mass generation in several classes of topological Dirac metals. We find that the dynamically generated masses manifest themselves as helical spin orders. These types of spin order have attracted considerable interests in other materials and models[35–40]. As we shall show, their emergence in topological Dirac (semi-)metal is a quite robust phenomenon, which is independent on material details. Physically, the helical spin orders result from the spin-orbit coupling. Their descriptions as Dirac fermions permits a unified treatment.

We present the results for three classes of materials. The first example is the edge state of quantum spin Hall (QSH) insulators[41–43]. Dynamically generated Dirac mass manifests itself as helical order at the edge [see Fig.1]. Quantum fluctuations, however, can destroy this order. Proximity to other materials (e.g. proximity to certain superlattice structures) can stabilize the helical order. The second example is the surface states of weak topological insulators, which are closely related to the first example, while avoiding the strong quantum fluctuations because of the higher dimensionality. The third example is Weyl semimetal in magnetic field. Here

the helical order depends on the direction of magnetic field in a specific manner, which provides a sharp experimental signature for identification of Weyl semimetals.

Helical order at QSH edge. The edge of QSH accommodate two counterpropagating modes, whose spin is locked with the propagating direction[44, 45]. The Hamiltonian reads

$$H(k) = \sum_k v_F(k - k_F) c_{\uparrow k}^\dagger c_{\uparrow k} - \sum_k v_F(k + k_F) c_{\downarrow k}^\dagger c_{\downarrow k} \quad (1)$$

where the chemical potential has been absorbed into the definition of k_F . This form of $H(k)$ is dictated by time reversal symmetry. We can introduce $c_{R/L}$ by $c_{\uparrow}(x) = e^{ik_F x} c_R(x)$ and $c_{\downarrow}(x) = e^{-ik_F x} c_L(x)$, then the Hamiltonian becomes

$$H(p) = v_F \sum_p p c_p^\dagger \sigma_z c_p, \quad (2)$$

where $c_p \equiv (c_{Rp}, c_{Lp})^T$ is the Fourier transformation of $c_{R/L}(x)$, and σ_z is the spin operator. This Hamiltonian describes a one-dimensional massless Dirac metal (more precisely, Weyl metal), with σ_z playing the role of chirality.

In this paper we focus on the possibility of dynamical fermion mass generation and symmetry breaking[46–48]. For simplicity let us take the interaction to be short-ranged, namely, $H_I = -g(c_L^\dagger c_R)(c_R^\dagger c_L)$ (with $g > 0$, which means repulsive interaction among electrons with opposite chirality). In the mean field theory, we define $m = g\langle c_L^\dagger c_R \rangle$, and obtain the mean field value of $|m|$ as

$$|m| = m_0 \equiv v_F \Lambda \exp\left(-\frac{2\pi v_F^2}{g}\right), \quad (3)$$

where Λ is a momentum cutoff. In this mean field calculation, only $|m|$ can be obtained, while the phase of m is arbitrary. It is convenient to write $m(x) = m_0 \exp(i\theta(x))$, neglecting the fluctuation of $|m|$. The ground state without Goldstone modes is $\theta(x) = \theta_0$, where θ_0 is an arbitrary real constant.

The expectation of the x -component of spin is given by

$$\begin{aligned} \langle \sigma_x(x) \rangle &= \langle c_{\uparrow}^\dagger(x) c_{\downarrow}(x) + c_{\downarrow}^\dagger(x) c_{\uparrow}(x) \rangle \\ &= e^{-iQx} \langle c_L^\dagger(x) c_R(x) \rangle + e^{iQx} \langle c_R^\dagger(x) c_L(x) \rangle \\ &= 2 \frac{m_0}{g} \cos(Qx - \theta(x)) \end{aligned} \quad (4)$$

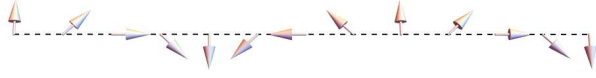


FIG. 1: Helical order at the edge of QSH.

where $Q \equiv 2k_F$. Similarly, we have

$$\begin{aligned} \langle \sigma_y(x) \rangle &= -ie^{-iQx} \langle c_L^\dagger(x) c_R(x) \rangle + ie^{iQx} \langle c_R^\dagger(x) c_L(x) \rangle \\ &= -2 \frac{m_0}{g} \sin(Qx - \theta(x)) \end{aligned} \quad (5)$$

and

$$\langle \sigma_z(x) \rangle = \langle c^\dagger(x) \sigma_z c(x) \rangle = \rho_R - \rho_L = 0 \quad (6)$$

The in-plane helical order is illustrated in Fig.(1). Finally, we remark that in 1D quantum fluctuations of Goldstone modes generally destroy the low-range order. The effect we have just found does not lose all significance, however, because of the following reasons. First, the helical order can persist if $2\pi/k_F$ is commensurate with the lattice constant (or the lattice constant of certain superlattice in proximity); secondly, the quasi-long-range helical order (power-law correlation of order) is measurable even if the true long-range order is absent.

Helical order at the surface of weak TI. A natural recipe to avoid strong quantum fluctuation in 1D is to couple many one-dimensional (1D) systems together to form a 2D system. This picture brings us to the study of this section.

Weak TIs are characterized by the so-called weak topological indices[49]. The simplest models of weak topological insulators consist of layered QSH [see Fig.2]. Therefore, the surface states can be obtained by coupling the QSH edge states. Suppose that the surface of the weak TI coincides with the xz -plane. To simplify the problem, we include hopping terms among only adjacent layers. The low energy Hamiltonian for the surface reads

$$\begin{aligned} H(\mathbf{k}) &= \sum_{\mathbf{k}} v_F(k_x - k_F) c_{\uparrow\mathbf{k}}^\dagger c_{\uparrow\mathbf{k}} - \sum_{\mathbf{k}} v_F(k_x + k_F) c_{\downarrow\mathbf{k}}^\dagger c_{\downarrow\mathbf{k}} \\ &\quad - 2t_{\parallel} \sum_{\mathbf{k}} \cos k_z (c_{\uparrow\mathbf{k}}^\dagger c_{\uparrow\mathbf{k}} + c_{\downarrow\mathbf{k}}^\dagger c_{\downarrow\mathbf{k}}), \end{aligned} \quad (7)$$

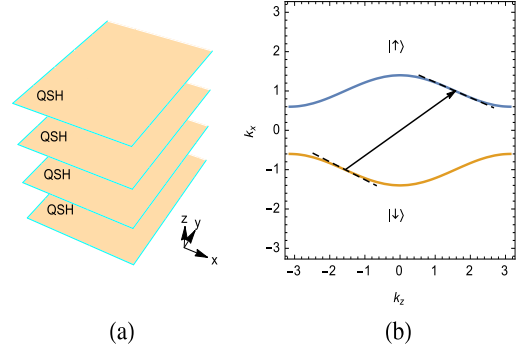
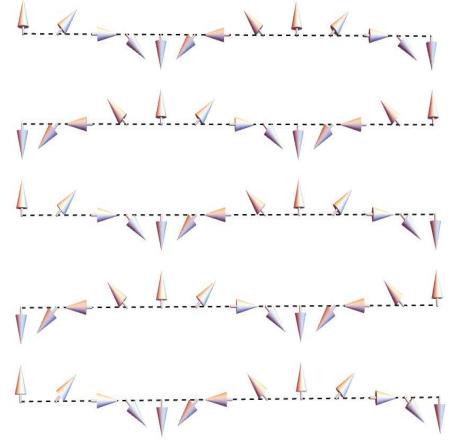
where $\mathbf{k} \equiv (k_x, k_z)$, and t_{\parallel} is the inter-layer hopping.

A notable feature of this Hamiltonian is as follows. The energy of electrons with spin up and spin down is $E_{\uparrow}(\mathbf{k}) = v_F(k_x - k_F) - 2t_{\parallel} \cos k_z$ and $E_{\downarrow}(\mathbf{k}) = -v_F(k_x + k_F) - 2t_{\parallel} \cos k_z$, respectively, therefore, we have

$$E_{\uparrow}(\mathbf{k} + \mathbf{Q}) = v_F(k_x + k_F) + 2t_{\parallel} \cos k_z = -E_{\downarrow}(\mathbf{k}) \quad (8)$$

where $\mathbf{Q} \equiv (2k_F, \pi)$. Therefore, there is perfect Fermi surface nesting at wavevector \mathbf{Q} . An infinitesimal interaction $H_I = -g(c_L^\dagger c_R)(c_R^\dagger c_L)$ can generate a gap, analogous to the case of QSH edge. The order parameter of this symmetry breaking is $m(\mathbf{x}) = g \langle c_L^\dagger(\mathbf{x}) c_R(\mathbf{x}) \rangle \equiv m_0 \exp(i\theta(\mathbf{x}))$. The spin densities are given by

$$\langle \sigma_x(\mathbf{x}) \rangle = \langle c_{\uparrow}^\dagger(\mathbf{x}) c_{\downarrow}(\mathbf{x}) + c_{\downarrow}^\dagger(\mathbf{x}) c_{\uparrow}(\mathbf{x}) \rangle$$

FIG. 2: (a) Weak TI as layered QSH. (b) Fermi surface nesting at the surface (in the xz plane) of weak TI.FIG. 3: Helical order at the surface of weak TIs. This spin order is helical in the x direction and antiferromagnetic in the z direction.

$$\begin{aligned} &= e^{-i\mathbf{Q} \cdot \mathbf{x}} \langle c_L^\dagger(\mathbf{x}) c_R(\mathbf{x}) \rangle + e^{i\mathbf{Q} \cdot \mathbf{x}} \langle c_R^\dagger(\mathbf{x}) c_L(\mathbf{x}) \rangle \\ &= 2 \frac{m_0}{g} \cos(\mathbf{Q} \cdot \mathbf{x} - \theta(\mathbf{x})) \end{aligned} \quad (9)$$

where $Q \equiv (2k_F, \pi)$, and

$$\begin{aligned} \langle \sigma_y(\mathbf{x}) \rangle &= -ie^{-i\mathbf{Q} \cdot \mathbf{x}} \langle c_L^\dagger(\mathbf{x}) c_R(\mathbf{x}) \rangle + ie^{i\mathbf{Q} \cdot \mathbf{x}} \langle c_R^\dagger(\mathbf{x}) c_L(\mathbf{x}) \rangle \\ &= -2 \frac{m_0}{g} \sin(\mathbf{Q} \cdot \mathbf{x} - \theta(\mathbf{x})) \end{aligned} \quad (10)$$

The spin texture at the weak TI surface is illustrated in Fig.3. The spin order is helical in the x direction, while antiferromagnetic in the z direction. Finally, we remark that inclusion of next-nearest-layer hopping destroys the perfect nesting, however, the picture we present should persist provided that the interaction strength is larger than these additional terms.

Helical spin order in Weyl semimetals. The dynamical mass generation induced by interaction and the resultant charge density wave state has been studied before[47, 48, 50–53]. With an external magnetic field, the Fermi surface instability becomes infinitesimal, i.e. an infinitesimal interaction can open up a gap at the Fermi surface[17, 54]. Charge density

wave pattern is, however, too crude to identify the unique feature of Weyl semimetals, namely, the spin-momentum locking described by the Weyl equation. Here we show the existence of helical spin orders, which provides a finer signature of Weyl-type spectrum.

For simplicity let us consider a single pair of Weyl points located at \mathbf{K}_1 and \mathbf{K}_2 respectively. We define the shorthand notation $\mathbf{Q} = \mathbf{K}_1 - \mathbf{K}_2$. The low-energy Weyl Hamiltonian reads $h_s(\mathbf{p}) = v_F \sum_{i,j=x,y,z} p_i e_{ij}^s \sigma_j$, in which $s = 1, 2$, $p_i \equiv k_i - K_{s,i}$, and e^s is a 3×3 matrix. For each $i = x, y, z$ we can define a vector $\mathbf{e}_i^s = (e_{ix}^s, e_{iy}^s, e_{iz}^s)$, thus h_s becomes more compact:

$$h_s(\mathbf{p}) = v_F \sum_{i=x,y,z} p_i (\mathbf{e}_i^s \cdot \boldsymbol{\sigma}), \quad (11)$$

where p_i is small compared to $|\mathbf{Q}|$. Hereafter we shall focus on the cases with $\mathbf{e}_i^s \cdot \mathbf{e}_j^s = \delta_{ij}$, for which compact analytical treatment is possible.

Now we add a magnetic field $\mathbf{B} = B\hat{z}$ (We can always rotate the coordinate system such that \mathbf{B} points in the \hat{z} direction)[66]. The energy eigenvalues for nonzero Landau levels are

$$E_l(p) = \pm v_F \sqrt{p_z^2 + 2eBl} \quad (l = 1, 2, 3, \dots) \quad (12)$$

which are all gapped. To obtain the zeroth Landau level, first we can solve the 2D problem in xy -plane by letting $p_z = 0$. In the Landau gauge the 2D Hamiltonian is

$$h_{2D}(q_x, q_y) = v_F [(p_x + eBy)\mathbf{e}_x^s \cdot \boldsymbol{\sigma} + p_y \mathbf{e}_y^s \cdot \boldsymbol{\sigma}]. \quad (13)$$

We can find that the zeroth Landau level wavefunction $\psi_{p_x}(x, y) = \frac{1}{\sqrt{2\pi eB}} \exp[-\frac{1}{2eB}(eBy + p_x)^2] \exp(ip_x x) |\mathbf{e}_x^s \times \mathbf{e}_y^s\rangle$, where we have introduced the notation $|\mathbf{n}\rangle$ to denote the two-component spinor satisfying $\langle \mathbf{n} | \sigma_i | \mathbf{n} \rangle = n_i$ for an vector \mathbf{n} . Adding the p_z term is now straightforward because $|\mathbf{e}_x^s \times \mathbf{e}_y^s\rangle$ is an eigenvector of $p_z \mathbf{e}_z^s \cdot \boldsymbol{\sigma}$ (This is the simplification of taking $\mathbf{e}_i^s \cdot \mathbf{e}_j^s = \delta_{ij}$). The single-particle wavefunction is

$$\psi_{p_x, p_z}^s(\mathbf{x}) = \frac{1}{\sqrt{2\pi eB}} \exp[-\frac{1}{2eB}(eBy + p_x)^2] \times \exp(ip_x x + ip_z z) |\chi_s \mathbf{e}_z^s\rangle, \quad (14)$$

in which we have introduced the chirality

$$\chi_s = (\mathbf{e}_x^s \times \mathbf{e}_y^s) \cdot \mathbf{e}_z^s = \pm 1, \quad (15)$$

and the single-particle energy is

$$E_{p_x, p_z}^s = v_F p_z \mathbf{e}_z^s \cdot \boldsymbol{\sigma} |\chi_s \mathbf{e}_z^s\rangle = \chi_s v_F p_z, \quad (16)$$

According to the above wavefunction structure, the fermion operators can be expanded as

$$c(\mathbf{x}) = \sum_s e^{i\mathbf{K}_s \cdot \mathbf{x}} |\chi_s \mathbf{e}_z^s\rangle c_s(\mathbf{x}) + \dots, \quad (17)$$

where “...” denotes high energy modes far away from the Weyl points. Suppose that $\chi_1 = -\chi_2 = 1$, then the index identification $1(2) \leftrightarrow R(L)$ is valid, and the analysis of dynamical symmetry breaking in the QSH section applies, namely, a four-fermion interaction induces a chiral condensation $\langle c_L^\dagger(\mathbf{x}) c_R(\mathbf{x}) \rangle = \frac{m(\mathbf{x})}{g} \equiv \frac{m_0}{g} \exp(i\theta(\mathbf{x}))$. The x -component of spin density becomes

$$\begin{aligned} \langle \sigma_x(\mathbf{x}) \rangle &= \langle c^\dagger(\mathbf{x}) \sigma_x c(\mathbf{x}) \rangle \\ &= e^{-i\mathbf{Q} \cdot \mathbf{x}} \frac{m(\mathbf{x})}{g} \langle \chi_2 \mathbf{e}_z^2 | \sigma_x | \chi_1 \mathbf{e}_z^1 \rangle + h.c. \end{aligned} \quad (18)$$

If we write $|\chi_1 \mathbf{e}_z^1\rangle = |\mathbf{e}_z^1\rangle = [\cos(\phi_1/2), \sin(\phi_1/2)e^{i\varphi_1}]^T$ and $|\chi_2 \mathbf{e}_z^2\rangle = |-\mathbf{e}_z^2\rangle = [\sin(\phi_2/2), -\cos(\phi_2/2)e^{i\varphi_2}]^T$, then we have $\langle \chi_2 \mathbf{e}_z^2 | \sigma_x | \chi_1 \mathbf{e}_z^1 \rangle = \sin(\phi_1/2) \sin(\phi_2/2) e^{i\varphi_1} - \cos(\phi_1/2) \cos(\phi_2/2) e^{-i\varphi_2}$. Similarly, we have

$$\begin{aligned} \langle \sigma_y(\mathbf{x}) \rangle &= \langle c^\dagger(\mathbf{x}) \sigma_y c(\mathbf{x}) \rangle \\ &= e^{-i\mathbf{Q} \cdot \mathbf{x}} \frac{m(\mathbf{x})}{g} \langle \chi_2 \mathbf{e}_z^2 | \sigma_y | \chi_1 \mathbf{e}_z^1 \rangle + h.c., \end{aligned} \quad (19)$$

with $\langle \chi_2 \mathbf{e}_z^2 | \sigma_y | \chi_1 \mathbf{e}_z^1 \rangle = -i[\cos(\phi_1/2) \cos(\phi_2/2) e^{-i\varphi_2} + \sin(\phi_1/2) \sin(\phi_2/2) e^{i\varphi_1}]$, and

$$\begin{aligned} \langle \sigma_z(\mathbf{x}) \rangle &= \langle c^\dagger(\mathbf{x}) \sigma_z c(\mathbf{x}) \rangle \\ &= e^{-i\mathbf{Q} \cdot \mathbf{x}} \frac{m(\mathbf{x})}{g} \langle \chi_2 \mathbf{e}_z^2 | \sigma_z | \chi_1 \mathbf{e}_z^1 \rangle + h.c., \end{aligned} \quad (20)$$

with $\langle \chi_2 \mathbf{e}_z^2 | \sigma_z | \chi_1 \mathbf{e}_z^1 \rangle = \cos(\phi_1/2) \sin(\phi_2/2) + \sin(\phi_1/2) \cos(\phi_2/2) e^{i(\varphi_1 - \varphi_2)}$. Finally, the charge density is

$$\begin{aligned} \langle \sigma_0(\mathbf{x}) \rangle &\equiv \langle c^\dagger(\mathbf{x}) c(\mathbf{x}) \rangle \\ &= e^{-i\mathbf{Q} \cdot \mathbf{x}} \frac{m(\mathbf{x})}{g} \langle \chi_2 \mathbf{e}_z^2 | \chi_1 \mathbf{e}_z^1 \rangle + h.c., \end{aligned} \quad (21)$$

with $\langle \chi_2 \mathbf{e}_z^2 | \chi_1 \mathbf{e}_z^1 \rangle = \cos(\phi_1/2) \sin(\phi_2/2) - \sin(\phi_1/2) \cos(\phi_2/2) e^{i(\varphi_1 - \varphi_2)}$.

Studying some special cases help us to understand these results. For instance, we consider

$$\begin{aligned} h_1(\mathbf{p}) &= v_F(p_x \sigma_x - p_y \sigma_z + p_z \sigma_y), \\ h_2(\mathbf{p}) &= v_F(p_x \sigma_x + p_y \sigma_z + p_z \sigma_y). \end{aligned} \quad (22)$$

It is readily seen that $\mathbf{e}_z^1 = \mathbf{e}_z^2 = (0, 1, 0)$, and the previous general results tell us that

$$\begin{aligned} \langle \sigma_x(\mathbf{x}) \rangle &= \frac{2m_0}{g} \sin(\mathbf{Q} \cdot \mathbf{x} - \theta(\mathbf{x})), \\ \langle \sigma_y(\mathbf{x}) \rangle &= 0, \\ \langle \sigma_z(\mathbf{x}) \rangle &= \frac{2m_0}{g} \cos(\mathbf{Q} \cdot \mathbf{x} - \theta(\mathbf{x})). \end{aligned} \quad (23)$$

This case is shown in Fig.(4a). If we take a different Weyl Hamiltonian

$$\begin{aligned} h_1(\mathbf{p}) &= v_F(p_x \sigma_x + p_y \sigma_y + p_z \sigma_z), \\ h_2(\mathbf{p}) &= v_F(p_x \sigma_x - p_y \sigma_y + p_z \sigma_z), \end{aligned} \quad (24)$$

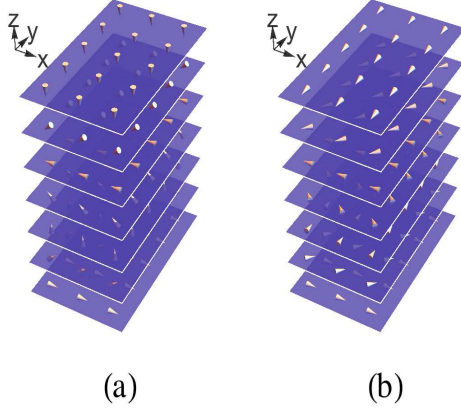


FIG. 4: Helical spin orders in Weyl semimetals with dynamical mass generation for (a) Hamiltonian in Eq.(22) and (b) Hamiltonian in Eq.(24). Here \mathbf{Q} is taken to be in the \hat{z} direction.

the a simple calculation yields

$$\begin{aligned}\langle\sigma_x(\mathbf{x})\rangle &= -\frac{2m_0}{g}\cos(\mathbf{Q}\cdot\mathbf{x}-\theta(\mathbf{x})), \\ \langle\sigma_y(\mathbf{x})\rangle &= -\frac{2m_0}{g}\sin(\mathbf{Q}\cdot\mathbf{x}-\theta(\mathbf{x})), \\ \langle\sigma_z(\mathbf{x})\rangle &= 0.\end{aligned}\quad (25)$$

This case is shown in Fig.(4b). The charge density $\langle\sigma_0(\mathbf{x})\rangle = 0$ for these two cases. Eq.(22) and Eq.(24) qualitatively resembles the Weyl semimetal materials and models. For instance, the simple model[17] $h(\mathbf{k}) = 2t_x \sin k_x \sigma_x + [2t_y(\cos k_y - \cos k_0) + m(2 - \cos k_x - \cos k_z)]\sigma_y + 2t_z \sin k_z \sigma_z$ has a pair of Weyl nodes at $(0, \pm k_0, 0)$, with $h_{s=1,2} = v_x \sigma_x p_x \pm v_y \sigma_y p_y + v_z \sigma_z p_z$ as its low-energy approximation, which is the same as Eq.(24) except for possible velocity anisotropy. More quantitative study of these materials shall be presented elsewhere.

By changing the direction of magnetic field, $|\mathbf{e}_z^s\rangle$ is changed accordingly, and the helical spin texture changes in a prescribed way. We also remark that if the Pauli matrices in Eq.(11) are not associated with spin but some other degrees of freedom, the helical order is a straightforward generalization of the above results.

The spin helix predicted here can be observed by spin-resolved scanning tunneling microscope (STM). It is unclear whether the magnitude of electron-electron interaction (and the sample quality) of the recently discovered Weyl semimetals favors generation of the spin helix, but we are probably justified to be optimistic about its possible realization, considering the ongoing rapid progress in this field.

Electric manipulation of spin texture. In the previous sections, we have focused on the cases $\theta(\mathbf{x}, t) = \theta_0$, which is independent on spacetime. The fluctuations of θ is certainly allowed in the general theory. These fluctuations are termed “axions”[55–57], and have also been studied in connection

to topological insulators[58, 59]. Similarly, the gravitational θ term and axions are useful in the description of topological superconductors[60–63]. In our present study the axion is much more visible because of their simple geometrical meaning: they are the phase angle of spin polarization (rotated from $\mathbf{Q}\cdot\mathbf{x}$).

Now we shall show that spin textures carry electric charge, moreover, the charge density depends on the spin texture in a precise manner. For concreteness, let us take the QSH edge as an example. In the presence of $\theta(\mathbf{x}, t)$, the spin polarization is pointing to angle $\mathbf{Q}\cdot\mathbf{x} - \theta(\mathbf{x}, t)$. Suppose that $\theta = \theta_0 - A \cos(qx)$, where $A \ll 1$ is the amplitude of spin modulation on the background of helical order. According to the Goldstone-Wilczek formula[64], we have

$$\rho(x) = \frac{1}{2\pi} \partial_x \theta = \frac{A}{2\pi} q \sin(qx). \quad (26)$$

On the other hand, if the charge density is given as $\rho(x) = \rho_0 \cos(qx)$, then we have

$$\theta(x) = \frac{2\pi\rho_0}{q} \sin(qx). \quad (27)$$

Therefore, gating the system periodically, such that the charge density modulates periodically, can control the spin modulation in a predictable manner.

We can also consider gating the system to induce a constant charge density $\rho_0(\mathbf{x}) = C$. According to the Goldstone-Wilczek formula, we have $\theta(\mathbf{x}) = 2\pi Cx$ for this case. Now the phase $\mathbf{Q}x - \theta(x) = (Q - 2\pi C)x$, namely, the wavevector of helical spin order becomes $Q - 2\pi C$. This is consistent with the relation $Q = 2k_F$: a constant charge density amounts to shifting k_F in the underlying Fermi surface “before” dynamical mass generation.

Finally, we remark that taking $k_F = 0$ brings us back to the result of Ref.[65], namely, a magnetic domain wall between $+x$ and $-x$ magnetization generates fractional charge $\pm e/2$. For a general $k_F \neq 0$, the $\pm x$ magnetization is replaced by spin helix with wavevector $Q = 2k_F$, i.e. both sides of the domain wall are spin helices, with a phase difference π .

Conclusions. A most prominent feature of topological Dirac and Weyl (semi-)metals is the spin-momentum locking, which is a dramatic consequence of spin-orbit coupling. We have shown that this spin-momentum locking can be “frozen” as helical spin ordering in the presence of dynamical instability (“helical solids” from helical liquids), which should be visible in spin-resolved STM. Apart from its intrinsic interest, it has potential application due to the electric tunability of helical order.

Acknowledgements. ZW is supported by NSFC under Grant No. 11304175 and Tsinghua University Initiative Scientific Research Program. SCZ is supported by the US Department of Energy, Office of Basic Energy Sciences under contract DE-AC02-76SF00515 and the NSF under grant numbers DMR-1305677.

* wangzhongemail@gmail.com

- [1] A. K. Geim and K. S. Novoselov, Nature materials **6**, 183 (2007).
- [2] X.-L. Qi and S.-C. Zhang, Physics Today **63**, 33 (2010).
- [3] M. Z. Hasan and C. L. Kane, Rev. Mod. Phys. **82**, 3045 (2010).
- [4] X.-L. Qi and S.-C. Zhang, Rev. Mod. Phys. **83**, 1057 (2011).
- [5] Z. Liu, B. Zhou, Y. Zhang, Z. Wang, H. Weng, D. Prabhakaran, S.-K. Mo, Z. Shen, Z. Fang, X. Dai, et al., Science **343**, 864 (2014).
- [6] M. Neupane, S.-Y. Xu, R. Sankar, N. Alidoust, G. Bian, C. Liu, I. Belopolski, T.-R. Chang, H.-T. Jeng, H. Lin, et al., Nature Communications **5**, 3786 (2014), 1309.7892.
- [7] S. Borisenko, Q. Gibson, D. Evtushinsky, V. Zabolotnyy, B. Büchner, and R. J. Cava, Phys. Rev. Lett. **113**, 027603 (2014), URL <http://link.aps.org/doi/10.1103/PhysRevLett.113.027603>.
- [8] X. Wan, A. M. Turner, A. Vishwanath, and S. Y. Savrasov, Phys. Rev. B **83**, 205101 (2011).
- [9] G. E. Volovik, *The Universe in a Helium Droplet* (Oxford University Press, USA, 2003).
- [10] A. A. Burkov and L. Balents, Phys. Rev. Lett. **107**, 127205 (2011), URL <http://link.aps.org/doi/10.1103/PhysRevLett.107.127205>.
- [11] A. A. Zyuzin, S. Wu, and A. A. Burkov, Phys. Rev. B **85**, 165110 (2012), URL <http://link.aps.org/doi/10.1103/PhysRevB.85.165110>.
- [12] W. Witczak-Krempa and Y. B. Kim, Phys. Rev. B **85**, 045124 (2012), URL <http://link.aps.org/doi/10.1103/PhysRevB.85.045124>.
- [13] P. Hosur, S. A. Parameswaran, and A. Vishwanath, Phys. Rev. Lett. **108**, 046602 (2012), URL <http://link.aps.org/doi/10.1103/PhysRevLett.108.046602>.
- [14] V. Aji, ArXiv e-prints (2011), 1108.4426.
- [15] C.-X. Liu, P. Ye, and X.-L. Qi, ArXiv e-prints (2012), 1204.6551.
- [16] G. Xu, H. Weng, Z. Wang, X. Dai, and Z. Fang, Phys. Rev. Lett. **107**, 186806 (2011), URL <http://link.aps.org/doi/10.1103/PhysRevLett.107.186806>.
- [17] K.-Y. Yang, Y.-M. Lu, and Y. Ran, Phys. Rev. B **84**, 075129 (2011), URL <http://link.aps.org/doi/10.1103/PhysRevB.84.075129>.
- [18] Z. Wang, Y. Sun, X.-Q. Chen, C. Franchini, G. Xu, H. Weng, X. Dai, and Z. Fang, Phys. Rev. B **85**, 195320 (2012), URL <http://link.aps.org/doi/10.1103/PhysRevB.85.195320>.
- [19] G. B. Halász and L. Balents, Phys. Rev. B **85**, 035103 (2012), URL <http://link.aps.org/doi/10.1103/PhysRevB.85.035103>.
- [20] J.-H. Jiang, Physical Review A **85**, 033640 (2012).
- [21] P. Delplace, J. Li, and D. Carpentier, ArXiv e-prints (2012), 1202.3459.
- [22] T. Meng and L. Balents, Physical Review B **86**, 054504 (2012).
- [23] I. Garate and L. Glazman, Phys. Rev. B **86**, 035422 (2012).
- [24] A. G. Grushin, ArXiv e-prints (2012), 1205.3722.
- [25] D. T. Son and B. Z. Spivak, ArXiv e-prints (2012), 1206.1627.
- [26] H. Weng, C. Fang, Z. Fang, B. A. Bernevig, and X. Dai, Phys. Rev. X **5**, 011029 (2015), URL <http://link.aps.org/doi/10.1103/PhysRevX.5.011029>.
- [27] L. Lu, Z. Wang, D. Ye, L. Ran, L. Fu, J. D. Joannopoulos, and M. Soljačić, ArXiv e-prints (2015), 1502.03438.
- [28] C. Zhang, Z. Yuan, S. Xu, Z. Lin, B. Tong, M. Zahid Hasan, J. Wang, C. Zhang, and S. Jia, ArXiv e-prints (2015), 1502.00251.
- [29] S.-Y. Xu, I. Belopolski, N. Alidoust, M. Neupane, C. Zhang, R. Sankar, S.-M. Huang, C.-C. Lee, G. Chang, B. Wang, et al., ArXiv e-prints (2015), 1502.03807.
- [30] B. Q. Lv, H. M. Weng, B. B. Fu, X. P. Wang, H. Miao, J. Ma, P. Richard, X. C. Huang, L. X. Zhao, G. F. Chen, et al., ArXiv e-prints (2015), 1502.04684.
- [31] X. Huang, L. Zhao, Y. Long, P. Wang, D. Chen, Z. Yang, H. Liang, M. Xue, H. Weng, Z. Fang, et al., ArXiv e-prints (2015), 1503.01304.
- [32] N. J. Ghimire, Y. Luo, M. Neupane, D. J. Williams, E. D. Bauer, and F. Ronning, ArXiv e-prints (2015), 1503.07571.
- [33] C. Shekhar, A. K. Nayak, Y. Sun, M. Schmidt, M. Nicklas, I. Leermakers, U. Zeitler, W. Schnelle, J. Grin, C. Felser, et al., ArXiv e-prints (2015), 1502.04361.
- [34] Y. Nambu and G. Jona-Lasinio, Phys. Rev. **122**, 345 (1961), URL <http://link.aps.org/doi/10.1103/PhysRev.122.345>.
- [35] O. Nakanishi, A. Yanase, A. Hasegawa, and M. Kataoka, Solid State Communications **35**, 995 (1980).
- [36] Y. Ishikawa, K. Tajima, D. Bloch, and M. Roth, Solid State Communications **19**, 525 (1976).
- [37] M. Uchida, Y. Onose, Y. Matsui, and Y. Tokura, Science **311**, 359 (2006).
- [38] B. Binz, A. Vishwanath, and V. Aji, Physical review letters **96**, 207202 (2006).
- [39] B. A. Bernevig, J. Orenstein, and S.-C. Zhang, Physical review letters **97**, 236601 (2006).
- [40] J. D. Koralek, C. Weber, J. Orenstein, B. Bernevig, S.-C. Zhang, S. Mack, and D. Awschalom, Nature **458**, 610 (2009).
- [41] C. L. Kane and E. J. Mele, Phys. Rev. Lett. **95**, 146802 (2005).
- [42] B. A. Bernevig, T. L. Hughes, and S.-C. Zhang, Science **314**, 1757 (2006).
- [43] M. König, S. Wiedmann, C. Brüne, A. Roth, H. Buhmann, L. Molenkamp, X.-L. Qi, and S.-C. Zhang, Science **318**, 766 (2007).
- [44] C. Wu, B. A. Bernevig, and S.-C. Zhang, Physical review letters **96**, 106401 (2006).
- [45] C. Xu and J. E. Moore, Physical Review B **73**, 045322 (2006).
- [46] E. Fradkin and J. E. Hirsch, Physical Review B **27**, 1680 (1983).
- [47] Z. Wang and S.-C. Zhang, Phys. Rev. B **87**, 161107 (2013), URL <http://link.aps.org/doi/10.1103/PhysRevB.87.161107>.
- [48] H. Wei, S.-P. Chao, and V. Aji, Physical Review Letters **109**, 196403 (2012), 1207.5065.
- [49] L. Fu, C. L. Kane, and E. J. Mele, Phys. Rev. Lett. **98**, 106803 (2007).
- [50] A. A. Zyuzin and A. A. Burkov, ArXiv e-prints (2012), 1206.1868.
- [51] J. Maciejko and R. Nandkishore, Phys. Rev. B **90**, 035126 (2014), URL <http://link.aps.org/doi/10.1103/PhysRevB.90.035126>.
- [52] R.-X. Zhang, J. A. Hutasoit, Y. Sun, B. Yan, C. Xu, and C.-X. Liu, ArXiv e-prints (2015), 1503.00358.
- [53] P. Buividovich, Physical Review D **90**, 125025 (2014).
- [54] B. Roy and J. D. Sau, ArXiv e-prints (2014), 1406.4501.
- [55] R. D. Peccei and H. R. Quinn, Phys. Rev. Lett. **38**, 1440 (1977), URL <http://link.aps.org/doi/10.1103/PhysRevLett.38.1440>.
- [56] F. Wilczek, Physical Review Letters **40**, 279 (1978).
- [57] S. Weinberg, Physical Review Letters **40**, 223 (1978).
- [58] X.-L. Qi, T. Hughes, and S.-C. Zhang, Phys. Rev. B **78**, 195424 (2008).
- [59] R. Li, J. Wang, X.-L. Qi, and S.-C. Zhang, Nature Physics **6**,

- 284 (2010).
- [60] Z. Wang, X.-L. Qi, and S.-C. Zhang, Phys. Rev. B **84**, 014527 (2011), URL <http://link.aps.org/doi/10.1103/PhysRevB.84.014527>.
- [61] S. Ryu, J. E. Moore, and A. W. W. Ludwig, Phys. Rev. B **85**, 045104 (2012), URL <http://link.aps.org/doi/10.1103/PhysRevB.85.045104>.
- [62] Z. Wang and S.-C. Zhang, Phys. Rev. B **86**, 165116 (2012), URL <http://link.aps.org/doi/10.1103/PhysRevB.86.165116>.
- [63] X.-L. Qi, E. Witten, and S.-C. Zhang, Physical Review B **87**, 134519 (2013).
- [64] J. Goldstone and F. Wilczek, Phys. Rev. Lett. **47**, 986 (1981).
- [65] X.-L. Qi, T. Hughes, and S.-C. Zhang, Nature Physics **4**, 273 (2008).
- [66] We focus on the orbital effects of magnetic field, omitting the Zeeman energy at this stage.